Clim Dyn (2016) 46:1185–1195
DOI 10.1007/s00382-015-2639-5

Investigation of the atmospheric mechanisms related to the autumn sea ice and winter circulation link in the Northern Hemisphere

Martin P. King[1] · Momme Hell[2,3] · Noel Keenlyside[4]

Received: 11 August 2014 / Accepted: 4 May 2015 / Published online: 13 May 2015

Abstract The relationship of Barents–Kara sea ice concentration in October and November with atmospheric circulation in the subsequent winter is examined using reanalysis and observational data. The analyses are performed on data with the 5-year running means removed to reduce the potential effects of slowly-varying external driving factors, such as global warming. We show that positive (negative) Barents–Kara sea ice concentration anomaly in autumn is associated with a positive (negative) North Atlantic Oscillation-like (NAO) pattern with lags of up to 3 months. The month-to-month variations in the lag relationships of the atmospheric anomalies related to November sea ice concentration are presented. Further analysis shows that the stratosphere-troposphere interaction may provide the memory in the system: positive (negative) sea ice concentration anomaly in November is associated with a strengthened (weakened) stratospheric polar vortex and these anomalies propagate downward leading to the positive (negative) NAO-like pattern in the late December to early January. This stratosphere mechanism may also play a role for Barents–Kara sea ice anomaly in December, but not for September and October. Consistently, Eliassen-Palm, eddy heat and momentum fluxes suggest that there is strong forcing of the zonal winds in November.

✉ Martin P. King
mki005@uni.no

[1] Uni Research, and Bjerknes Centre for Climate Research, Allegaten 70, 5007 Bergen, Norway

[2] GEOMAR, University of Kiel, Kiel, Germany

[3] Present Address: ETH, Zurich, Switzerland

[4] Geophysical Institute, University of Bergen, and Bjerknes Centre for Climate Research, Allegaten 70, 5007 Bergen, Norway

Keywords Climate impact of Arctic sea ice · Sea ice-atmosphere interaction · North Atlantic Oscillation · Stratosphere downward propagation

1 Introduction

As the Arctic sea ice experiences large changes in the recent decades, many studies are being conducted to investigate the impacts of sea ice on Northern Hemisphere climate, in particular in the summer to winter seasons. These studies have been based on observations and model results, and have investigated recent as well as possible future changes.

The relationships of atmospheric anomalies in autumn and winter to Arctic sea ice in the preceding late summer (August and September) have been examined by applying various statistical analysis on atmospheric reanalysis and observational data (Francis et al. 2009; Hopsch et al. 2012; Jaiser et al. 2012). In September, the largest variance in sea ice concentration (SIC) is found to be in region of the Laptev, East Siberian, and Beaufort seas (90°–210°E) (e.g. see Ogi and Wallace 2007; Hopsch et al. 2012). In general, it was found that a circulation anomaly pattern similar to the negative (positive) North Atlantic Oscillation (NAO) phase is associated with low (high) sea ice in the summer. Hopsch et al. (2012), however, caution that the areas with statistical significance tend to be limited.

The results from the recent studies appear consistent with those of earlier atmospheric general circulation model (AGCM) studies investigating the climate impact of sea ice variability or projected future sea ice loss (e.g. Alexander et al. 2004; Magnusdottir et al. 2004; Seierstad and Bader 2009; Deser et al. 2010; King et al. 2010). In general, these showed negative NAO response in late winter (February

or March), while the largest sea ice loss is in late summer to autumn. The link between winter atmospheric circulation and late summer to autumn sea ice changes remains unclear. There is ongoing research using various later-generation AGCMs to investigate the robustness of the response and its consistency across different models and background climates.

Honda et al. (2009) and Inoue et al. (2012) focus on the impact of September SIC off the Russian coast (30°E–180°) on winter climate in Eurasia. They found that in observations an anomalously low (high) SIC is associated with below- (above-) average surface temperature in eastern Eurasia. They were also able to reproduce similar responses in wintertime (as late as February) in AGCM idealised experiments driven with anomalous SIC prescribed from September to December. Evidence presented suggests that turbulent heat flux associated with sea ice differences perturb a stationary Rossby wave over Eurasia. At these latitudes, Rossby waves are well developed within a month and so the cause of the delayed response well into February was unclear.

One hypothesis for the dynamics or 'memory' in the system for the winter atmospheric response to autumn or late summer sea ice condition is that persistent anomalous diabatic heating and meridional temperature gradient excite and maintain an anomalous NAO state, through changes in low-level baroclinicity (e.g. Francis et al. 2009). Stratosphere-troposphere interaction could also play a role (Orsolini et al. 2012; Jaiser et al. 2012; Garcia-Serrano et al. 2014; Kim et al. 2014). The specific aim of this study is better understand the possible role of stratosphere-troposphere interaction in linking changes in autumn sea ice and winter atmospheric circulation.

We apply conventional methods to further investigate the statistical relationships in reanalysis and observational data (described in Sect. 2) between autumn (October and November) sea ice in the Barents and Kara (denoted BK hereafter) seas and the atmospheric anomalies in autumn to winter (December–February). We focus on October and November BK SIC, rather than September or earlier months in the Arctic area of 90°–210°E as used in many previous studies. This relationship between late autumn and winter has been studied less, but is more robust and may have a clearer linkage mechanism. We analyse interannual variability rather than the low-frequency changes which can confound the identification of physical mechanisms in the short period for which high-quality sea ice data are available. Interannual variability explains almost 50 % of the variance in the BK SIC in autumn and understanding the mechanisms on this timescale can be useful for understanding longer time scale changes, as well as of relevance for seasonal prediction (e.g. Balmaseda et al. 2010; Fereday et al. 2012; Orsolini et al. 2012). Section 3 presents the results from month-to-month analyses, and analysis that suggests stratosphere-troposphere interaction provides part of the memory in the system that links the two seasons. Discussion and conclusions are given in Sect. 4.

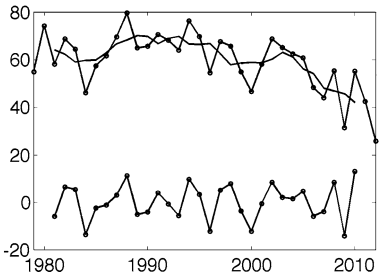

Fig. 1 Area-average Barents SIC (%) time series for November (*upper line* with *circle* markers); its 5-year running mean is the line without markers. The anomalous Barents SICs with the 5-year running mean removed (tSIC) is shown as the *lower line*. Original data are from NSIDC

2 Data and methodology

This study utilises data from the National Snow and Ice Data Center (NSIDC, Cavalieri et al. 1996) and the NCEP-NCAR Reanalysis (Kalnay et al. 1996). The variables included sea ice concentration, geopotential heights, near-surface temperature (at sigma level = 0.995) and others. The period of 1979–2012 for which the NSIDC data are available is the focus. This period provides reliable reanalysis and observational data, especially for the sea ice. We have repeated many analyses presented in the following sections using ERA-INTERIM data, namely the ones involving geopotential heights and air temperature. It was found that analyses using ERA-INTERIM data produce nearly identical results to those using NCEP-NCAR Reanalysis.

The SIC time series used in the linear regression calculations are defined as the monthly mean area-averaged SIC in the 0°–90°E, 75°–85°N area (BK seas) with their 5-year running means removed. Figure 1 shows, as an example, the November SIC time series in BK seas from 1979 to 2012; its 5-year running mean; and tSIC, the anomalous SIC time series with the 5-year running mean removed. All analyses are carried out on monthly-mean or 5-day-mean data with their 5-year running means removed. The variances of the year-to-year SIC fluctuations (i.e. for the time series with the 5-year running mean removed) are 40–50 % of the total SIC variances in October and November. Therefore, in addition to the long-term sea ice loss, the year-to-year variability of sea ice could play an important part in the Northern Hemisphere climate. The impacts of global warming and other low-frequency climate drivers make it

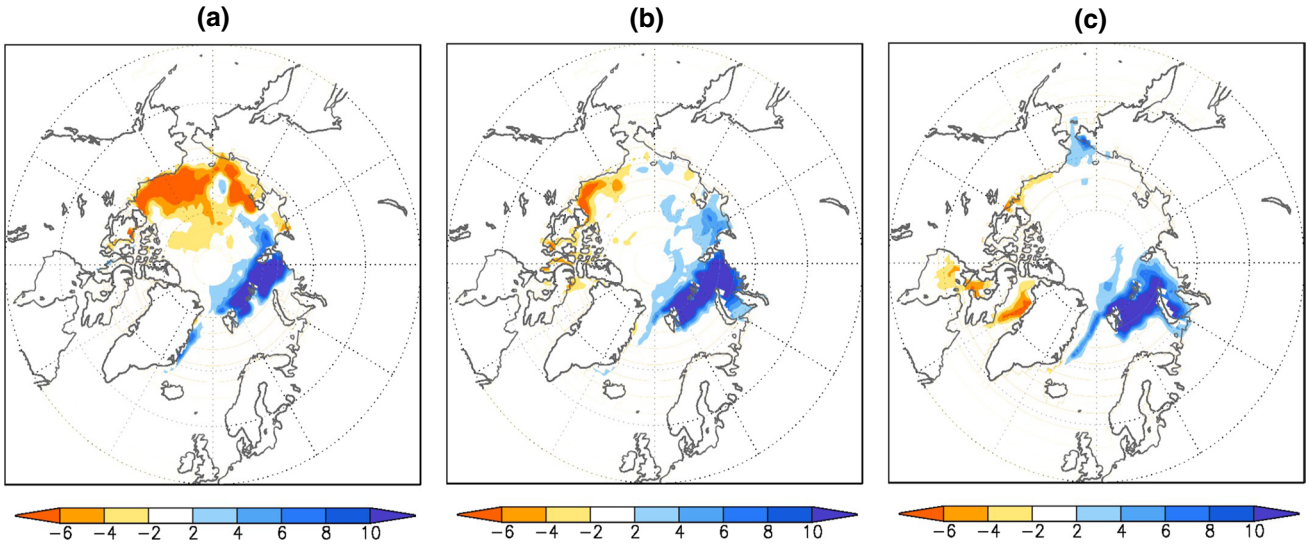

Fig. 2 Regressions of sea ice concentration (SIC, %) in September, October and November on the Barents sea ice concentration time series (tSIC) for the respective months. Data from NSIDC for 1979–2012. **a** Sep SIC and Sep tSIC. **b** Oct SIC and Oct tSIC. **c** Nov SIC and Nov tSIC

difficult to estimate robust statistical relationships in the relatively short satellite period. Thus, removing low-frequency variability and trends increases the statistical power of our analyses (Ogi and Wallace 2007).

Many previous studies investigating impacts of sea ice on the atmosphere used data with the best-fit straight line removed (i.e. detrend; e.g. Ogi and Wallace 2007; Francis et al. 2009; Hopsch et al. 2012). We repeated analyses on data with 3- or 7-year running means removed and found that the widths of the running means do not strongly influence our results. Further tests repeated using spectral filtering, with frequencies lower than 1 cycle per 5 years removed, found that the linear regressions obtained have weaker amplitudes than the ones from data with the running means removed. For the most extreme differences, there are locations that are up to 50 % weaker; however in most areas the differences are no more than 30 %. Furthermore, the thresholds of the spectral filtering (comparing high-pass filtering using 1 cycle per 5 years, 1 cycle per 7 years, and 1 cycle per 10 years thresholds) do not have a strong influence on the results, which remain statistically significant. In summary, we have tested our approach to isolate the interannual variability and found that our results do not depend strongly on the exact method to remove low-frequency variations.

The tSIC index characterises quite different variability in October and November compared to September, as shown by the regressions of Arctic SIC on tSIC for the respective months (Fig. 2). In September, SIC variability occurs in a large area over the Arctic ocean; while the October and November SIC variability is mainly limited to the BK seas. Furthermore, in September, sea ice variations in BK seas are associated with fluctuation of the opposite sign in the other parts of the Arctic. Note that the current paper presents the SIC anomaly signs as in conventional statistics, rather than inverting them (i.e. multiplied the reference time series by −1) to display the results from the perspective of the long-term sea ice loss like in many recent papers. We use cold colours to represent positive SIC anomaly and warm colours for negative SIC anomaly. The regressions of the atmospheric variables to tSIC for October or November presented in Sect. 3 are associated with the SIC spatial variability and amplitudes shown in Fig. 2.

3 Results and discussion

3.1 The relation of autumn sea ice concentration with the winter atmospheric circulation

Analyses show that late autumn SIC in the BK seas is more strongly related to the winter atmospheric circulation anomaly in the North Atlantic sector, compared with concurrent large-scale circulation. To illustrate the point, Fig. 3 shows the regressions of SIC, near-surface temperature (TAS) and 500 hPa geopotential heights (Z500), for October–November (ON) and December-January–February (DJF), on the October–November mean tSIC. The DJF Z500 pattern in the North Atlantic sector that is linked to ON tSIC (Fig. 3f) has a meridional dipole structure similar to NAO but with the centres shifted northward. There is corresponding large surface temperature anomaly over Eurasia (Fig. 3e). In contrast, TAS and Z500 patterns in ON are weaker and less significant (Fig. 3b, c). The impact on

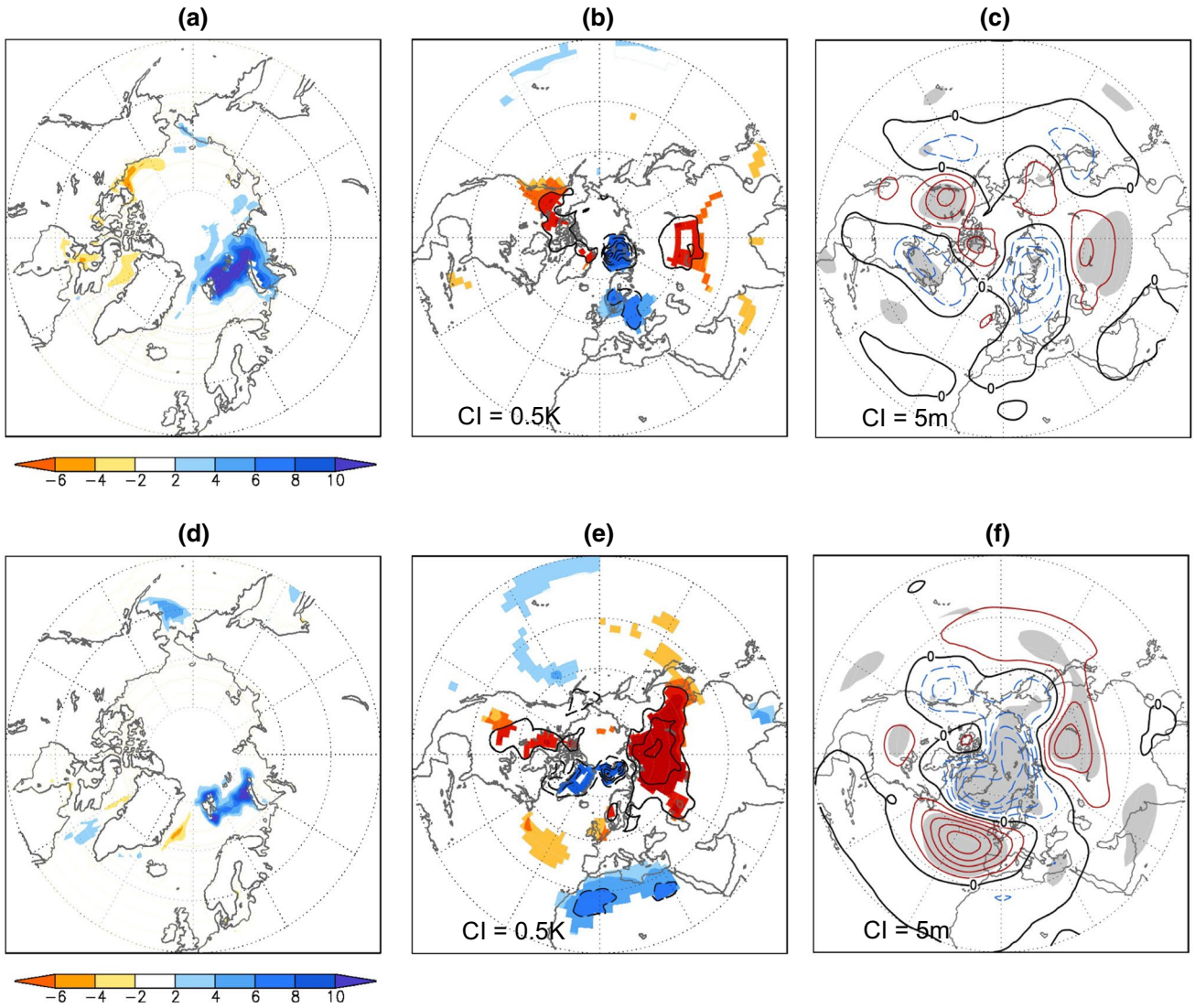

Fig. 3 Regressions of Oct–Nov (top row) and Dec–Jan–Feb (*bottom row*) mean SIC (%), near-surface temperature (TAS) and 500 hPa geopotential heights (Z500) on the Oct-Nov mean Barents Sea SIC time series. Solid contours represent positive values; dashed contours negative values in *middle* and *right* panels. Shaded area indicates 95 % statistical significance. CI is contour interval. Data from NSIDC and NCEP/NCAR Reanalysis for 1979–2012. **a** OctNov SIC and OctNov tSIC. **b** OctNov TAS and OctNov tSIC. **c** OctNov Z500 and OctNov tSIC. **d** DJF SIC and OctNov tSIC. **e** DJF TAS and OctNov tSIC. **f** DJF Z500 and OctNov tSIC

Eurasian temperature (Fig. 3e), which has been noted by previous studies (e.g. Honda et al. 2009), amplifies in the winter months. The response and feedback with the atmosphere of this particular temperature anomaly needs further investigation (and is not in the scope of the present paper). The persistence of the sea ice forcing is one potential explanation for the linkage between autumn sea ice and winter atmospheric circulation anomalies, and there is indeed persistence of SIC anomalies in ON to DJF (Fig. 3d; however see also result below).

AGCM experiments prescribed with positive (negative) SIC anomalies in DJF in the BK seas area can excite the positive (negative) NAO phase in DJF (see references as given in Introduction). Thus, results from these studies and Fig. 3 are consistent with the suggestion that the persistence of SIC anomaly from autumn to winter and the associated turbulent heat flux from the adjacent ocean area can be responsible for the connection of autumn sea ice and winter circulation revealed by statistical analyses. In a recent study, Liptak and Strong (2014) used realistic daily varying Barents sea ice anomalies to force the Community Atmosphere Model (CAM version 4) for wintertime (December–February). However, both their anomalous low and high sea ice cases produced negative NAO responses in February. The responses of the AGCMs to sea ice anomalies in winter require more

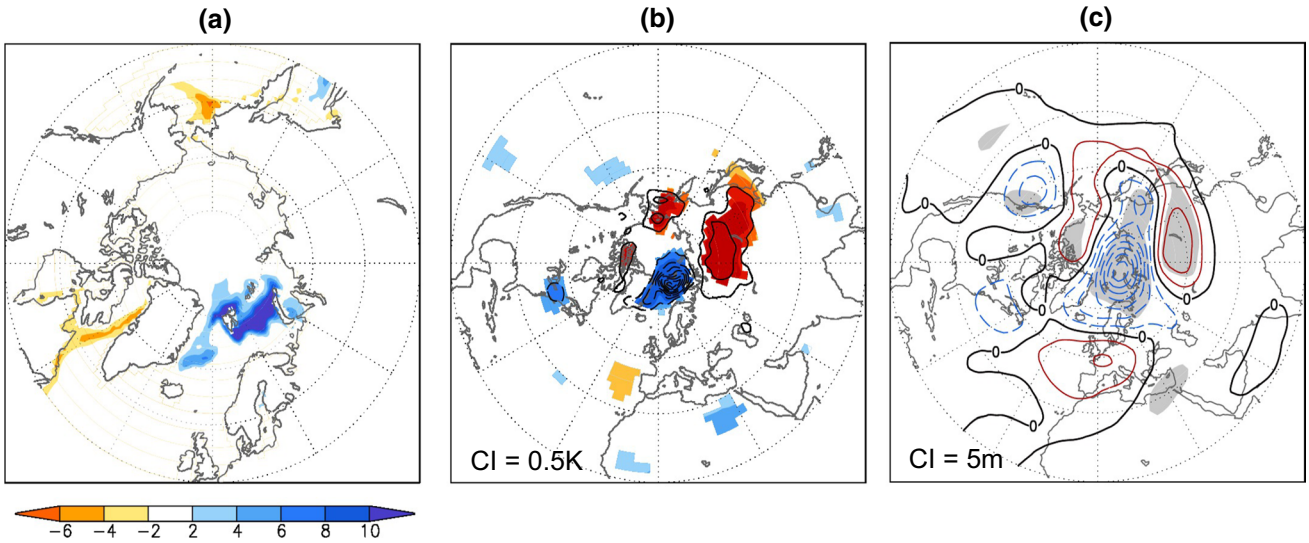

Fig. 4 Regressions of DJF mean sea ice concentration (SIC, %), DJF mean TAS, and DJF mean Z500 on the DJF Barents Sea SIC time series. Solid contours represent positive values; dashed contours negative values in panels **b** and **c**. Shaded area indicates 95 % statistical significance. Data from NSIDC and NCEP/NCAR Reanalysis for 1979–2012. **a** DJF SIC and DJF tSIC. **b** DJF TAS and DJF tSIC. **c** DJF Z500 and DJF tSIC

research particularly concerning model and mean flows dependencies.

The winter atmospheric circulation pattern related to winter SIC anomalies, however, differs substantially to that with autumn SIC anomalies. Specifically, the relationship between tSIC in DJF and Z500 in DJF is not an NAO-like pattern, as well as not having statistical significant relationship in a large part of the North Atlantic (see Fig. 4c). This indicates that, when winter seasonal means are considered, the dominant statistical relationship does not arise from SIC exciting the NAO (contrary to what is believed to be the case, as discussed above), but may either indicate that a different pattern is excited or that the atmosphere is forcing the SIC. Thus, sea ice persistence from autumn to DJF alone (Fig. 3d) cannot explain the mean DJF atmospheric response (Fig. 3f). Nevertheless, the response in the Eurasia region remains robust and similar to that linked to ON SIC (compare Fig. 4b, c with Fig. 3e, f). Strong et al. (2009) and Frankignoul et al. (2014), however, did find that at sub-seasonal timescale (e.g. in order of weeks), sea ice and NAO are in lead-lag negative feedback relationships.

Other studies have indicated that the persistence of sea ice might not be the main mechanism for the amplification of the response in late winter. In particular, Honda et al. (2009) demonstrated in their AGCM experiments that the delayed response in both the North Atlantic and Eurasia sectors continues until at least February even though the anomalous SIC is only applied from September to December (other months have climatological SIC and SST conditions). While there may be yet other factors for the Eurasia part of the response, such as the feedback from the snow cover (which is also a topic of active research), the origin of the North Atlantic response in late winter is unclear, particularly as SIC anomalies are absent in January and February (Honda et al. 2009).

To better understand the possible causes for the relation of the winter atmospheric circulation to autumn sea ice anomalies (Fig. 3), we examine the relation of SIC in November with the monthly atmospheric anomalies. Shown in Fig. 5 are the monthly regressions of TAS, Z500 and Z50 from November to February on tSIC in November. Between October and November, the November month is chosen somewhat arbitrarily here, however analyses in the following subsection indicate that the atmospheric perturbations related to sea ice in November are particularly strong. For TAS, a response of opposite sign is found over Eurasia/Russia to that directly over the sea ice. This anomaly weakened somewhat in December (Fig. 5b) but picks up again in January and February (Fig. 5c, d). This phenomenon is potentially predictable (see for e.g. Garcia-Serrano et al. 2014) and can partially arise from the downward propagation of stratospheric anomalies. The atmospheric signals have a lag of up to 3 months from November. The associated spatial pattern for Z500 in the North Atlantic sector has a meridional dipole structure that resembles the NAO, but with their centres shifted to the north somewhat (Fig. 5f, g, h), that is well-developed in January and February. At the upper level, Z50 anomalies (Fig. 5i–k) linked to positive (negative) tSIC anomaly in November project onto a strengthening (weakening) of the Northern Annular Mode

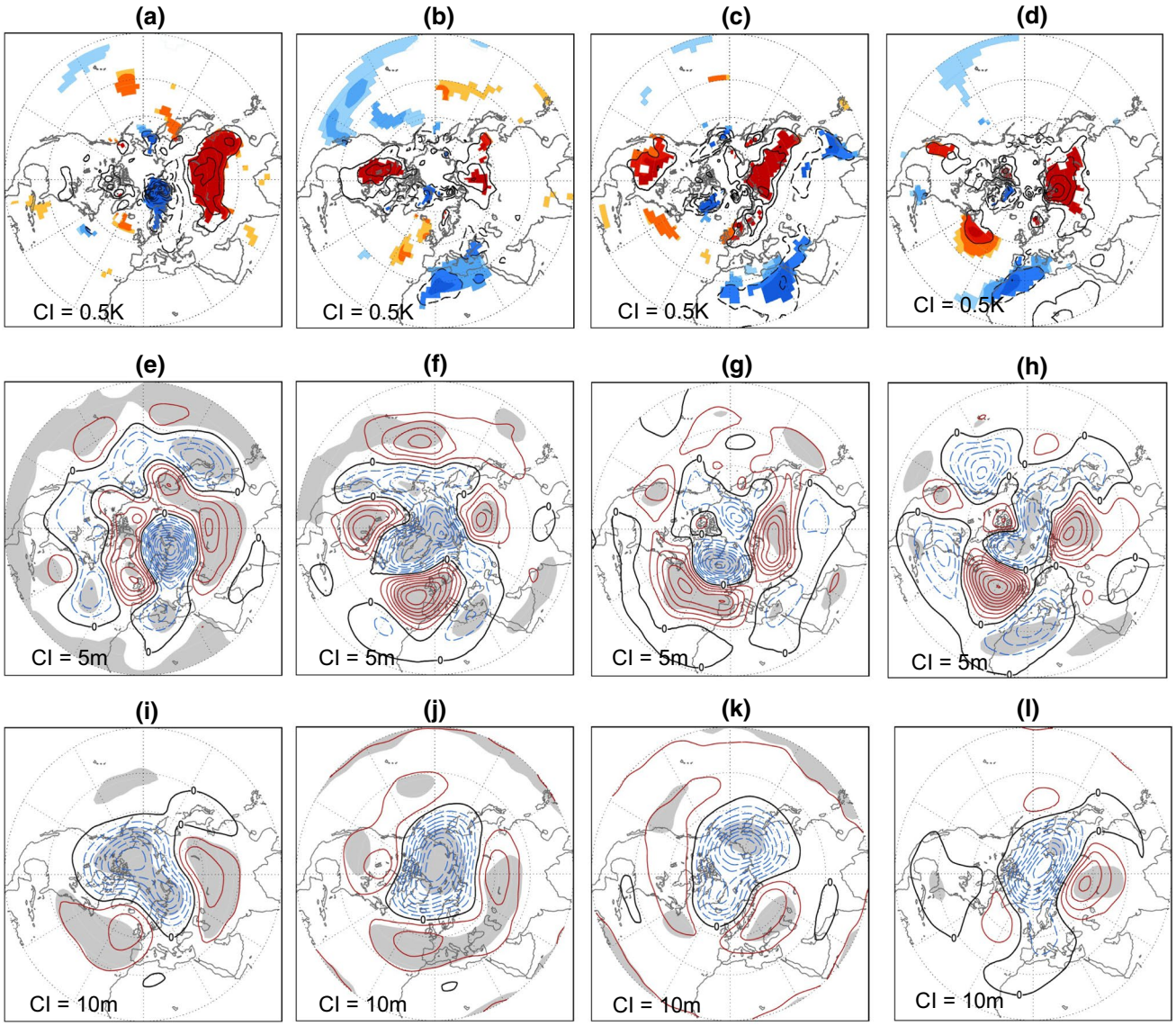

Fig. 5 Regressions of the fields shown in November, December, January, and February on the November Barents Sea SIC time series. Solid contours represent positive values; dashed contours negative values. *Shaded* area indicates 95 % statistical significance. Data from NSIDC and NCEP/NCAR reanalysis for 1979–2012. **a** Nov TAS and Nov tSIC. **b** Dec TAS and Nov tSIC. **c** Jan TAS and Nov tSIC. **d** Feb TAS and Nov tSIC. **e** Nov Z500 and Nov tSIC. **f** Dec Z500 and Nov tSIC. **g** Jan Z500 and Nov tSIC. **h** Feb Z500 and Nov tSIC. **i** Nov Z50 and Nov tSIC. **j** Dec Z50 and Nov tSIC. **k** Jan Z50 and Nov tSIC. **l** Feb Z50 and Nov tSIC

(NAM). In the next subsection, the time evolution of this anomaly across the vertical levels is investigated.

3.2 Role of the stratosphere

There has been a suggestion that stratosphere-troposphere interaction can contribute to linking late summer and early autumn sea ice with the winter circulation anomalies. Jaiser et al. (2013) investigated the stratospheric change in DJF that has been concurrent with the long-term Arctic sea ice reduction in August and September in recent decades. They reported that a weakening polar vortex and warmer stratospheric temperature (related to negative phase of Arctic Oscillation) are linked to low ice conditions. Orsolini et al. (2012) speculated on the role of the stratosphere in bridging September sea ice and late winter circulation anomalies through downward propagation. Cohen et al. (2007) proposed, with supporting analyses, a similar role of the stratosphere in bridging Eurasian snow cover in October and polar troposphere geopotential heights in the subsequent winter. Besides the persistence in SIC, sea surface temperature and land-surface properties, the stratospheric polar vortex, which has a fairly long decorrelation time up to 2 months (e.g. Baldwin and Dunkerton 2001),

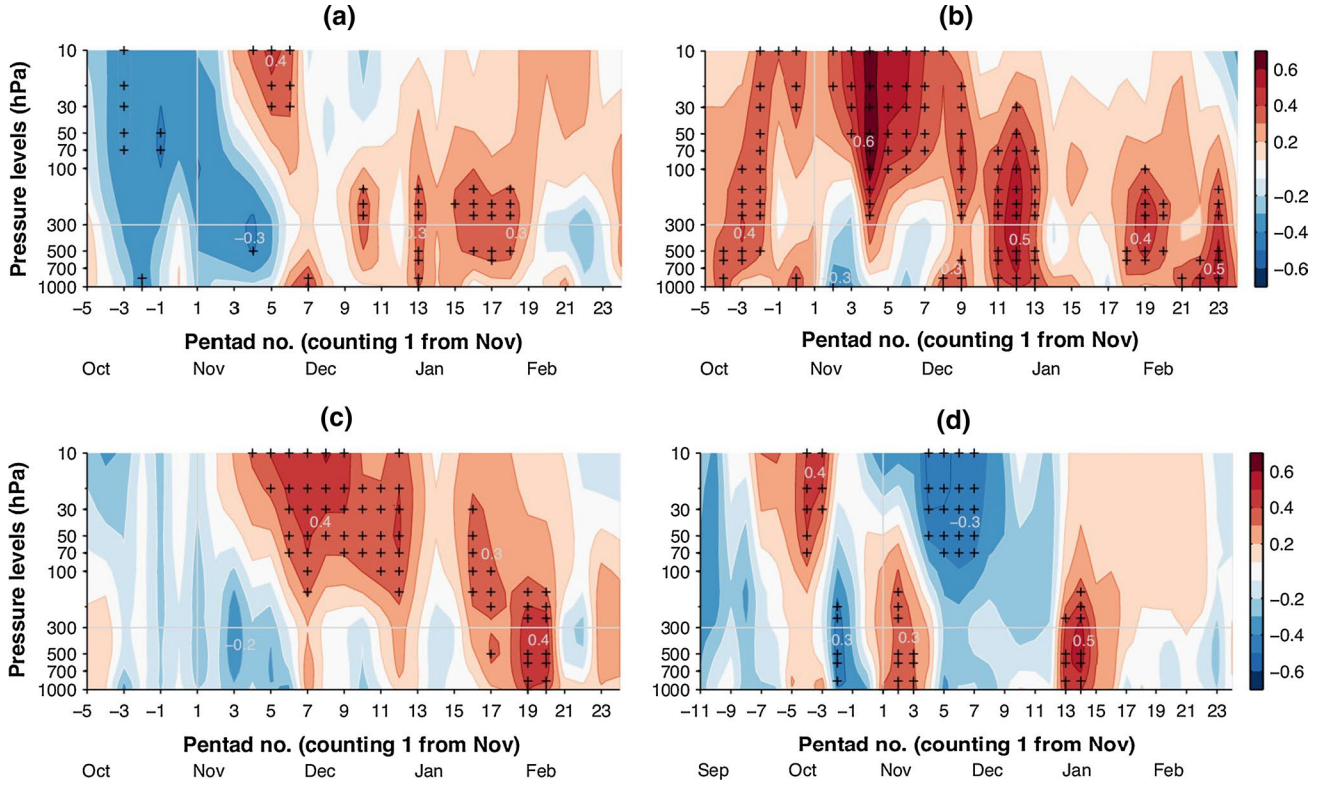

Fig. 6 Correlation coefficients of NAM index and Barents SIC time series for **a** October, **b** November, **c** December, and **d** with September SIC time series for the Laptev to Beaufort sea areas. Contour interval = 0.1. The crosses mark values of statistical significance at 95 %. Pentad number 1 is the first 5 days of November, pentad number 0 is the 5 days prior to first day of November, and so on such that the x axis is from October–February in **a**–**c**; and September–February in **d**. Data from NCEP/NCAR Reanalysis and NSIDC for 1979–2012

is another potential factor in providing a 'memory' in the interactions.

To examine the roles of the lower stratosphere and upper troposphere in linking sea ice in autumn and the winter atmosphere, we calculate the correlation coefficients between the NAM index at different vertical levels from October to February and reference tSIC for October, November, and December, respectively (Fig. 6a, b, c). The NAM index here is calculated as the normalised area-averaged geopotential height in the zonal band of 40°–60°N minus the same of 70°–90°N, on 5-day (pentad) mean data. The 5-day means for NAM are used here, instead of monthly means, in order to better capture the NAM temporal evolution. The pentads numbering is explained in the caption of Fig. 6.

The tropospheric signals from December to January (pentads no. 7–18) are particularly strongly related to tSIC of November (Fig. 6b). More importantly, these tropospheric signals appear to be preceded by anomalies in the upper troposphere and lower stratosphere. Correlations of NAM and tSIC of December (Fig. 6c) also shows hint of the downward propagation relationship between stratospheric anomaly in December and tropospheric anomaly in mid-January–mid-February (pentads no. 16–21). In contrast, the tropospheric signals in December–January that are related to October sea ice anomaly have a weaker relation to preceding stratospheric NAM anomalies. The stratospheric mean-flow variation can induce divergence of eddy momentum fluxes or Rossby waves in such a way that flow anomalies are directed poleward and downward. Explanations of the NAM downward propagation can be found in Baldwin and Dunkerton (2001), Thompson et al. (2003), and Omrani et al. (2014). The phenomenon of the stratosphere-troposphere downward propagation is well accepted although the mechanisms are not yet completely understood (Omrani et al. 2014 and references therein). The tropospheric NAM signals in February linked to November tSIC (Fig. 6b) do not appear to be connected directly to the stratosphere, but could result from the persistence of surface forcings or be a manifestation of the lead-lag negative feedback relationship between sea ice and the atmosphere (Strong et al. 2009 and Frankignoul et al. 2014).

The NAM correlations with tSIC defined for September using the area 90°–210°E, 70°–85°N do not show the signature of NAM downward propagation signature from September stratosphere to the troposphere in the winter months

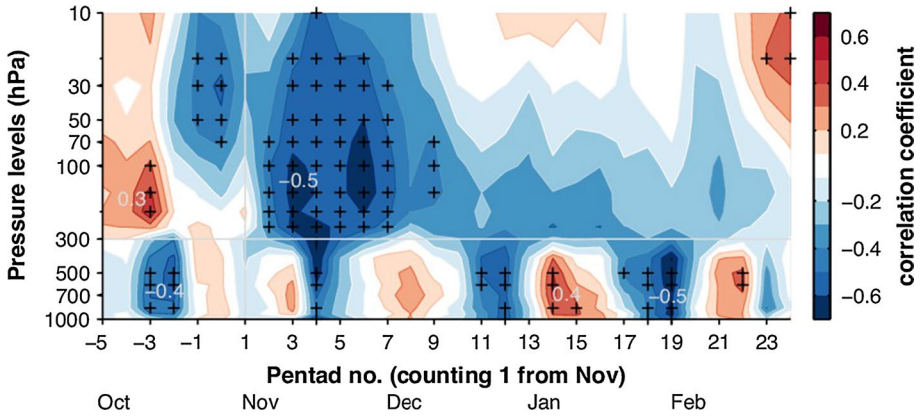

Fig. 7 Correlation coefficients of polar air temperature (area-average poleward of 70°N) and tSIC in November. Contour interval = 0.1. The crosses mark values of statistical significance at 95 %. Pentad number 1 is the first 5 days of November, pentad number 0 is the 5 days prior to first day of November, and so on such that the x axis is from October–February. Data from NCEP/NCAR reanalysis and NSIDC for 1979–2012

(Fig. 6d). This particular area of SIC used is the location of strong SIC variability in September, and also the area used in analyses of previous studies (e.g. Hopsch et al. 2012). The significant lagged correlations imply that the relation of tropospheric anomalies (e.g. in January during pentads no. 13–18) with September SIC may be due to persistence in surface forcings, and not related to interaction involving higher levels of the atmosphere. Calculations that have been repeated using the ERA-INTERIM data produced similar results to Fig. 6.

The analysis using NAM index is somewhat restrictive, as the atmosphere has other modes of variability and its responses to sea ice forcings (e.g. see Fig. 5) might differ from the NAM. Therefore, we also computed the correlation coefficients between the area-averaged polar air temperature (poleward of 70°N) and tSIC for November (Fig. 7). For the purpose here, the polar air temperature may be a good alternative to NAM index because it is a variable that can be related to more than just NAM or NAO circulations. Other modes of variability such as the Scandinavian and the cold-ocean-warm-land patterns are able to drive the polar air temperature as well. Related to positive (negative) tSIC, there is cold (warm) air column throughout the upper atmosphere in November, with an indication of downward propagation in the subsequent months (Fig. 7). Intervals of up to 15–20 days with alternating signs are seen in the lower part of the troposphere (to about 500 hPa) which could be a signature of the negative feedbacks between sea ice and atmosphere (Strong et al. 2009).

3.3 Analyses of eddy and Eliassen-Palm fluxes

To help understand the particularly strong connection between November sea ice and stratospheric variations, we examine the transient and quasi-stationary eddy activity related to BK sea ice variations in the months from October to December. Anomalous eddy activity is able to drive changes in the NAO and NAM (e.g. Limpasavun and Hartmann 2000, and similar diagnostics by Seierstad and Bader 2009). Here we compute the regressions of eddy fluxes of heat (v*T*) at the 925 hPa level and momentum (u*v*) at the 200 hPa level on tSIC for October, November, and December (Fig. 8). These levels chosen are the locations of large climatological eddy fluxes. The asterisk indicates deviations from the zonal means; and ten-day low-pass spectral filter has been applied first to the daily u*, v*, and T* so that planetary waves in the barotropic timescales are retained. The monthly means are then calculated from the daily values of eddy fluxes.

The eddy heat and momentum fluxes that are linked to tSIC are larger in November than in October (Fig. 8; note the larger contour interval in panel d). In November, the eddy heat flux at the 925 hPa level is strong over the BK seas, Scandinavia, and northern Russia (Fig. 8c), while there are poleward eddy momentum fluxes over Europe and the North Pacific near Japan (Fig. 8d). The negative anomalous eddy heat flux over the North Atlantic remains strong in December (Fig. 8e). In the zonal mean, u*v* and v*T* are related to the horizontal and vertical components respectively of the Eliassen-Palm flux (EP flux, Edmon et al. 1980). The anomalous negative v*T* over Scandinavia (Fig. 8c, e) is indicative of suppression of vertical propagation of planetary waves (e.g. see the diagnostics of Nishii et al. 2011), and the convergence of u*v* in northern Europe and near Japan (Fig. 8d) are consistent with the Z50 anomaly (Fig. 5i) and implies strengthening of zonal symmetry and zonal wind.

We next use EP flux diagnostic to show the differences in the forcings of the zonal-mean zonal flow by eddies in a formalised way. Here, we follow exactly the formulations given by Edmon et al. (1980). In the latitude φ and pressure p components respectively, the EP flux is defined to be $r\cos\varphi\,[-(u^*v^*), f\,(v^*\theta^*)/\theta_p]$, where the square bracket denotes zonal mean, r is the Earth's radius, f is Coriolis parameter, θ is potential temperature, and θ_p is the partial derivative with respect to p. Linear regression is used to identify the relation of tSIC with EP flux, its divergence, and zonal-mean zonal wind in October, November, and

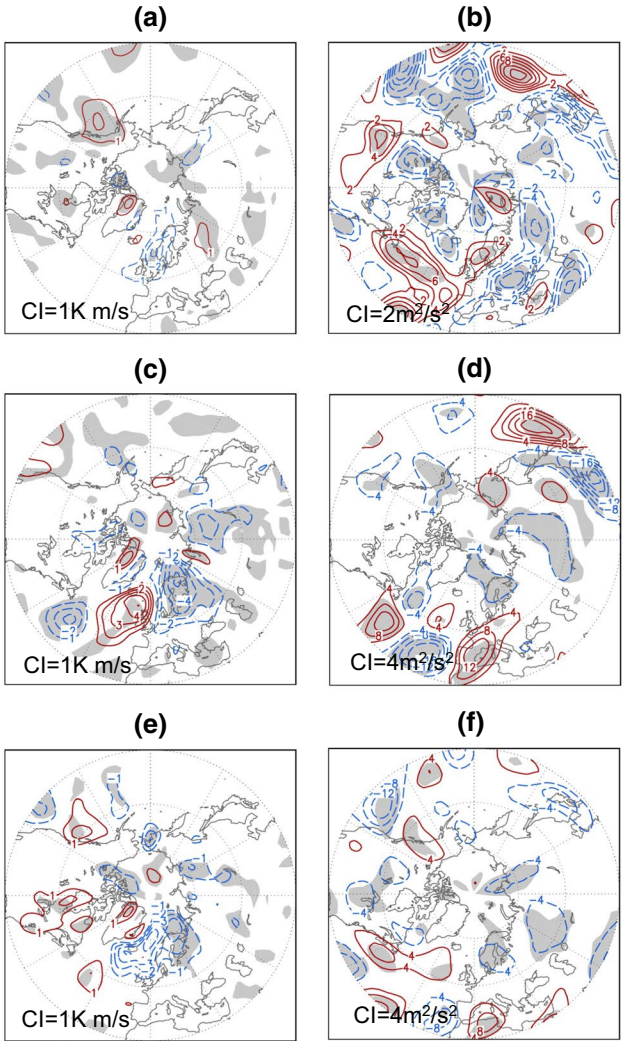

Fig. 8 Regressions of meridional eddy heat flux at 925 hPa (*left*) and eddy momentum flux at 200 hPa (*right*) on Barents SIC time series for October (*top*), November (*middle*), and December (*bottom*). *Shaded area* indicates 95 % statistical significance. Tenday low-pass filtering has been applied first on daily u*, v* and T*. The 5-year running means are then removed from the monthly eddy fluxes data. Data from NCEP/NCAR Reanalysis and NSIDC for 1979–2012. **a** Oct v*T* and Oct tSIC. **b** Oct u*v* and Oct tSIC. **c** Nov v*T* and Nov tSIC. **d** Nov u*v* and Nov tSIC. **e** Dec v*T* and Dec tSIC. **f** Dec u*v* and Dec tSIC

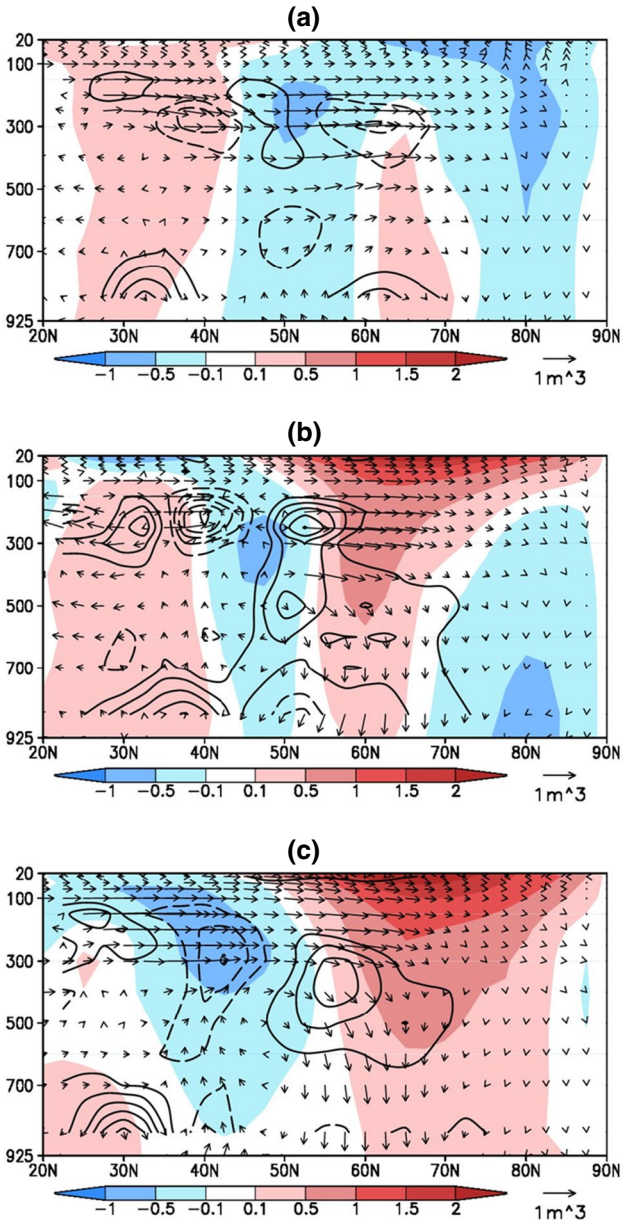

Fig. 9 Regressions of EP flux [vectors, in units of $m^3(10^{13}$ rad, 10^{19} Pa)]; divergence of EP flux (CI = $0.5 \times 10^{14} m^3$, contours); and zonal mean zonal wind U (m/s, colour shading) on Barents SIC time series for the respective months of **a** October, **b** November, and **c** December. Data from NCEP/NCAR reanalysis and NSIDC for 1979–2012. **a** Oct EPFLUX; DIV; U. **b** Nov EPFLUX; DIV; U. **c** Dec EPFLUX; DIV; U

December (Fig. 9). We also scale the EP vectors to be displayed appropriately on a latitude-pressure plane according to Edmon et al. (1980), and this leads to the 'unusual' units in Fig. 9. It is also important to note that the pressure coordinate in the vertical axis requires that positive (negative) values for vertical components of the EP flux vectors are pointing downward (upward) (Edmon et al. 1980).

In November and December, at around 60°N, and up to about 500 hPa, BK sea ice anomaly is associated anomalous eddy heat fluxes (vertical EP flux), while at higher levels at about 200 hPa anomalous eddy momentum fluxes (horizontal EP flux) dominates, as indicated by the relative directions of the vectors (Fig. 9b, c). The overall effect is such that for high SIC anomaly, the anomalous EP fluxes cancel the climatological ones, thus weakening the eddies propagations. In the transformed zonal mean flow with quasi-geostrophic approximation, the divergence of the EP flux is the only internal forcing resulting from the atmospheric disturbances (eddies) on the acceleration of the

zonal flow. In December (Fig. 9c), there are areas of EP flux divergence at the middle to upper troposphere; while the EP flux divergence for November (Fig. 9b) is somewhat stronger and exists in larger vertical extent. The case for October (Fig. 9a), however, shows the absence of eddy heat flux and the presence of very weak EP flux divergence at the upper level. These EP flux diagnostics support the more active role for stratosphere-troposphere interaction in November.

4 Summary and conclusions

In this paper we examine the relationships between the Barents–Kara (BK) sea ice in autumn with the subsequent winter atmospheric circulation by analysing data from NCEP/NCAR Reanalysis and NSIDC. The main aims of the study are to better understand the physical mechanisms linking the winter atmosphere with autumn sea ice variations, as well as to identify month-to-month variations in the lag relationship of the atmosphere with the autumn sea ice. In particular, the potential role of the stratosphere-troposphere interaction in the observed lag relationship between the two seasons is investigated.

Significant large-scale atmospheric signals with a lag of up to 3 months are found to follow BK sea ice anomaly in November. The positive (negative) anomalous BK sea ice in November is associated with Z500 in the North Atlantic sector which has a meridional dipole structure resembling the positive (negative) NAO in January and February, but with its centres shifted to the north somewhat (see panels f, g, h in Fig. 5). For the near-surface temperature, at two- to three-months lags, a strong impact appears over land in northern Russia, Siberia and North America regions (see panels c, d in Fig. 5).

The tropospheric signals in December–January which are linked to BK sea ice in November are preceded by NAM signals in the lower stratosphere that propagate downward (Fig. 6b). This relation is less apparent for October sea ice and not present for September. Analysis using polar air temperature (area-averaged poleward of 70°N) at different atmospheric levels also shows the same signature, with anomalies of the same sign in the whole atmospheric column in November that propagate downward from the top to lower atmosphere in the subsequent months (Fig. 7). The signal is punctuated by intervals of alternating signs lasting about 15–20 days in the lower levels in December–February. This may be a result of the negative feedback reported by Strong et al. (2009) or simply due to the shorter timescales of NAM in the troposphere (Thompson et al. 2003). Analysis of eddy diagnostics provide further evidence that November, rather than earlier months, is the month in which stratosphere-troposphere interaction is most active in linking autumn BK sea ice with the winter circulation.

Our results add to the findings of two recent studies. Garcia-Serrano et al. (2014) reported similar result on the downward propagation using ERA-Interim data, although their study focuses on the predictability aspect. They reported that the November Barents sea ice provides significant cross-validated predictability skill for the subsequent winter atmosphere. While Kim et al. (2014) also reported the role of the stratosphere and downward propagation in the relationship of low sea ice and the atmosphere, it appears that their composite analyses using Nov–Dec low sea ice years detected strong upper level signals only from mid-January. Additionally, their model experiment contains anomalous sea ice perturbations in all months, therefore their study may be more related to the winter season srelationships.

Our analysis indicates that the September SIC relationships with winter NAO reported by a number of previous studies (see Introduction) cannot be explained by the stratosphere NAM linkage. However, there is still a statistically significant NAM correlation in January in the troposphere (thus also highly correlated with NAO). This could result from persistence or feedbacks with surface forcings which requires further investigation.

Although it is tempting at this point to suggest that the SIC in autumn ‘causes’ the subsequent wintertime atmospheric anomalies, we believe that the question about causality is not fully settled. For example, the eddy meridional heat flux over northern Europe shown in Fig. 8c can be a result of positive SIC anomaly, or equally this negative anomalous eddy heat flux is causing the positive SIC anomaly; both are feasible physically. The coupled interaction between sea ice and atmosphere involves complicated lead-lag feedbacks. Improvement in understanding requires the use of models. However, a main challenge is that the fidelity of climate models to simulate the processes and relationships among the processes is not well known and needs to be investigated comprehensively.

Acknowledgments The NCEP-NCAR Reanalysis data are provided by NOAA/OAR/ESRL PSD, Boulder, Colorado, USA (http://www.esrl.noaa.gov/psd). The sea ice concentration (Cavalieri et al. 1996) data are from the National Snow and Ice Data Center, USA. The work was supported by the GREENICE project, funded by the NordForsk Top-level Research Initiative (Project no. 61841). We acknowledge fruitful discussion with Hisashi Nakamura and Javier Garcia-Serrano on this study. We thank the two reviewers for their comments which had led to improvements of this paper.

References

Alexander MA, Bhatt US, Walsh JE, Timlin MS, Miller JS, Scott JD (2004) The atmospheric response to realistic Arctic sea ice anomalies in an AGCM during winter. J Clim 17:890–905

Baldwin MP, Dunkerton TJ (2001) Stratospheric harbinger of anomalous weather regimes. Science 294:581–584

Balmaseda MA, Ferranti L, Molteni F, Palmer TN (2010) Impact of 2007 and 2008 Arctic ice anomalies on the atmospheric circulation: implications for long-range predictions. Q J R Meteorol Soc 136:1655–1664

Cavalieri DJ, Parkinson CL, Gloersen P, Zwally H (1996) Sea ice concentration from Nimbus-7 SMMR and DMSP SSM/I-SSMIS passive microwave data. NASA DAAC at the National Snow and Ice Data Center, Boulder

Cohen J, Barlow M, Kushner P, Saito K (2007) Stratosphere-troposphere coupling and links with Eurasian land surface variability. J Clim 20:5335–5343

Deser C, Tomas R, Alexander M, Lawrence D (2010) The seasonal atmospheric response to projected Arctic sea ice loss in the late twenty-first century. J Clim 23:333–351. doi:10.1175/2009JCLI3053.1

Edmon HJ, Hoskins BJ, McIntyre ME (1980) Eliassen-Palm cross-sections for the troposphere. J Atmos Sci 37:2600–2616

Fereday DR, Maidens A, Arribas A, Scaife AA, Knight JR (2012) Seasonal forecasts of northern hemisphere winter 2009/10. Environ Res Lett 7:034031. doi:10.1088/1748-9326/7/3/034031

Francis JA, Chan W, Leathers DJ, Miller JR, Veron DE (2009) Winter northern hemisphere weather patterns remember summer Arctic sea-ice extent. Geophys Res Lett 36:L07503. doi:10.1029/2009GL037274

Frankignoul C, Sennechael N, Cauchy P (2014) Observed atmospheric response to cold season sea ice variability in the Arctic. J Clim 27:1243–1254. doi:10.1175/JCLI-D-13-00189.1

Garcia-Serrano J, Frankignoul C, Gastineau G, de la Camara A (2014) On the predictability of the winter Euro-Atlantic climate: lagged influence of autumn Arctic sea ice. J Clim. doi:10.1175/JCLI-D-14-00472.1

Honda M, Inoue J, Yamane S (2009) Influence of low Arctic sea-ice minima on anomalously cold Eurasian winters. Geophys Res Lett 36:L08707. doi:10.1029/2008GL037079

Hopsch S, Cohen J, Dethloff K (2012) Analysis of a link between Arctic sea ice concentration and atmospheric patterns in the following winter. Tellus A 64:18264. doi:10.3402/tellusa.v64i0.18624

Inoue J, Hori ME, Takaya K (2012) The role of Barents sea ice in the wintertime cyclone track and emergence of a warm-Arctic cold-Siberian anomaly. J Clim 25:2561–2568. doi:10.1175/JCLI-D-11-00449.1

Jaiser R, Dethloff K, Handorf D, Rinke A, Cohen J (2012) Impact of sea ice cover changes on the Northern Hemisphere atmospheric winter circulation. Tellus A 64:11595. doi:10.3402/tellusa.v64i0.11595

Jaiser R, Dethloff K, Handorf D (2013) Stratospheric response to Arctic sea ice retreat and associated planetary wave propagation changes. Tellus A 65:19375. doi:10.3402/tellusa.v65i0.19375

Kalnay E et al (1996) The NCEP/NCAR 40-year reanalysis project. Bull Am Meteorol Soc 77:437–470

Kim B-M et al (2014) Weakening of the stratospheric polar vortex by Arctic sea-ice loss. Nat Commun. doi:10.1038/ncomms5646

King MP, Kucharski F, Molteni F (2010) The roles of external forcings and internal variabilities in the Northern Hemisphere atmospheric circulation change from the 1960s to the 1990s. J Clim 23:6200–6220. doi:10.1175/2010JCLI3239.1

Limpasavun V, Hartmann DL (2000) Wave-maintained annular modes of variability. J Clim 13:4419–4429

Liptak J, Strong C (2014) The winter atmospheric response to sea ice anomalies in the Barents Sea. J Clim 27:914–924. doi:10.1175/JCLI-D-13-00186.1

Magnusdottir G, Deser C, Saravanan R (2004) The effects of North Atlantic SST and sea ice anomalies on the winter circulation in CCM3. Part I: main features and storm track characteristics of the response. J Clim 17:857–876

Nishii K, Nakamura H, Orsolini YJ (2011) Geographical dependence observed in blocking high influence on the stratospheric variability through enhancement and suppression of upward planetary-wave propagation. J Clim 24:6408–6423. doi:10.1175/JCLI-D-10-05021.1

Ogi M, Wallace JM (2007) Summer minimum Arctic sea ice extent and the associated summer atmospheric circulation. Geophys Res Lett 34:L12705. doi:10.1029/2007GL029897

Omrani NE, Keenlyside N, Bader J, Manzini E (2014) Stratosphere key for wintertime atmospheric response to warm Atlantic decadal conditions. Clim Dyn 42:649–663. doi:10.1007/s00382-013-1860-3

Orsolini YJ, Senan R, Benestad RE, Melsom A (2012) Autumn atmospheric response to the 2007 low Arctic sea ice extent in coupled ocean-atmosphere hindcasts. Clim Dyn 38:2437–2448. doi:10.1007/s00382-011-1169-z

Seierstad IA, Bader J (2009) Impact of a projected future Arctic sea ice reduction on extratropical storminess and the NAO. Clim Dyn 33:937–943. doi:10.1007/s00382-008-0463-x

Strong C, Magnusdottir G, Stern H (2009) Observed feedback between winter sea ice and the North Atlantic Oscillation. J Clim 22:6021–6032. doi:10.1175/2009JCLI3100.1

Thompson DWJ, Lee S, Baldwin MP (2003) Atmospheric processes governing the Northern Hemisphere annular mode/North Atlantic Oscillation. In: The North Atlantic Oscillation: Climatic Significance and Environmental Impact. Geophys Monogr Ser 134:81-112. doi: 10.1029/134GM05